복합재 평판 내부에 삽입된 광섬유 브래그 격자 센서의 삽입안전성과 신호 특성에 관한 연구

이정률* · 류치영* · 강현규* · 김대현* · 구본용** · 강동훈* · 홍창선*** · 김천곤***

The Embedding Reliability and The Spectrum Characteristic of Fiber Bragg Grating Sensor Embedded into Composite Laminates

Jungryul Lee, C. Y. Ryu, H. K. Kang, D. H. Kim, B. Y. Koo, D. H. Kang, C. S. Hong and C. G. Kim

KEY WORDS : Birefringence, FBG, Embedding reliability, Spectrum characteristics, WSFL, Cure monitoring, Residual stress

ABSTRACT

FBGs have been extensively used as strain sensors or temperature sensors in a variety of applications related to composites because of embedding ability, small size and multiplexing capability. We inspected embedding environments inside composites with optical fiber by microscope analysis and birefringence characteristics of FBG embedded into textile composite laminate by cure monitoring using a high power WSFL. The cure monitoring of the cases with the striped FBG and the recoated FBG provided comprehensive understandings about the birefringence effect induced by the transverse stress. And these results allowed to consider a recoating method as an important tool to relieve birefringence.

NOMENCLATURE

SMF : Single Mode optical Fiber
FBG : Fiber Bragg Grating
WSFL : Wavelength Swept Fiber Laser
WSFLWI : WSFL Wavelength Indicator
ASE : Amplified Spontaneous Emission
FP : Fabry Perot
Lo-Bi : Low Birefringence
Hi-Bi : High Birefringence
SOP : State Of Polarization
DPO : Digital Phosphor Oscilloscope
OSA : Optical Spectrum Analyzer
LP_{01} : Linearly Polarized mode (or HE_{11})

1. INTRODUCTION

FBG sensors can be embedded in advanced composites and other materials to measure internal strain, temperature and other parameters. The first application of fiber gratings was an embedded strain sensor in an epoxy-fiber composite laminate[1].

These small, highly sensitive sensors have been demonstrated in many applications with aids of the development of the higher speed demodulation method and the multiplexing technique[2]. One of the high-speed demodulation systems was developed as employing the high power WSFL, WSFLWI and FP filter[3]. The FBG sensor system could measure dynamic strains real-timely as the signal processing circuit converting the peaks into the digital pulse train was introduced to the FBG sensor system [4].

In 1995, it had been noticed that stress induced birefringence effects in Lo-Bi fibers can cause the unique Bragg condition to break down[5]. This phenomenon was used another development of FBG strain sensor, what is called, 2-D strain field measurement sensor. Although FBG sensors were used to measure longitudinal and transverse strain quantitatively using Lo-Bi fiber or Hi-Bi fiber, this distortion of unique Bragg condition have caused some ambiguity to measure dynamic strains because of two split peaks. Especially when FBG strain sensor is embedded into composite structures, the inherent residual stress after cure processing may induce birefringence of FBG.

Microbendings cause light losses and backscatters optically and can lead to stress fractures mechanically. In the application of FBG embedded in composites aspect, mechanical microbending effects are more important than optical microbending effects relatively. Therefore it should be checked whether optical fibers under uneven embedding environments of composite materials with different microbendings can have the mechanical embedding reliability after cure processing or not, as well as optical embedding reliability of FBG as dynamic strain sensor.

* 한국과학기술원 항공우주공학과 대학원
** 도남시스템㈜
*** 한국과학기술원 항공우주공학과

For several situations and cases of composite laminates, we inspected optical and mechanical reliability of optical fiber built in FBG for measurement of dynamic strain. And we performed cure-monitoring experiments in order to understand the characteristics of sensor spectra related to the residual stress induced birefringence.

2. FBG as STRAIN SENSOR

Fabrication of FBG sensor

A FBG is a periodic and refractive index perturbation that is formed inside the core of an optical fiber exposed by an intense UV interference pattern. The technique for stable grating fabrication in this study could be achieved using a phase mask as shown in Fig. 1 and associated equipments (KrF eximer laser and 3-axis translation stage and so on). Broadband light incident on the grating is reflected back a slightly narrow band with the Bragg resonance wavelength. Because the core is a homogeneous isotropic medium optically for a SMF, the Bragg condition including this resonance wavelength can represent by using the effective index, n_e=1.4476

$$\lambda_B = 2n_e\Lambda \quad (1)$$

In this paper, the effective index of the fiber core was acquired from pitches of the phase mask and the reflective Bragg wavelengths after writing

Coating of optical fiber

SMF consists of a germanium-doped core for a slightly high refraction and a silica cladding. The standard diameter of telecommunication fibers is 125 μm . A coating increases diameter to about 250 μm , easing handling and protecting fiber surfaces from scratches and other mechanical damage. Optical fibers used in this study have double coatings. This dual protective acrylate coating is applied over the fiber cladding to cushion the fiber against optical microbending effects, to provide abrasion resistance, and to preserve the mechanical strength of the silica. In general, the coating of optical fiber should be stripped to build grating in an optical fiber using a KrF excimer laser and a phase mask. Therefore a stripped FBG was recoated using the same material (acrylate) by VYT-200-C in this study.

FBG sensor system

When strains are to be measured by using an FBG sensor, it is important to detect Bragg wavelength shift exactly. The resolution of FBG sensor system is also momentous for acquiring the spectrum of birefringent FBGs which have split peaks. For these facts, the WSFL-DPO FBG sensor system was employed in this study. The WSFL has an FP filter which is driven by periodic triangular waveform to produce a wavelength sweep over 40 nm from 1525 to 1565 nm. The laser output is launched into the sensing gratings and the reference grating for temperature compensation. In addition, it is possible to monitor the cure processing of composite materials without any special treatment by the WSFL-DPO FBG sensor system in spite of serious microbending problems inside an autoclave and at its door part. This is reason why the average output power (2.22mW) of WSFL is over 1000 times as large as that of ASE.

LED-OSA FBG sensor system was used in this study to estimate initial wavelengths of a reference FBG and sensing FBGs. Also, this system was useful to understand changes in FBG spectra simply.

The resolution of these two systems depends on measuring instruments. DPO used in this study detects peak as narrow as 1ns, therefore the resolution of WSFL-DPO FBG sensor system whose laser source output is converted into electric signal by a low-speed detector is 0.00033 nm . While the resolution of OSA used in this study is 0.071 nm .

Birefringence of an embedded FBG sensor

Ideal SMF preserve the SOP of input light. In practice, however, optical fibers do not behave ideally, but show birefringence. This birefringence is caused by the following reasons.

(1) Slightly elliptical optical fiber core.
(2) Intrinsic stress in an optical fiber.
(3) Transverse stress.
(4) Bending of an optical fiber.

(1), (2) are classified the intrinsic birefringence and it present in the optical fiber because of built-in anisotropies, either intentional or not. (3), (4) are classified the induced birefringence. When an optical fiber is bent with host composite material, birefringence introduced due to both an asymmetrical transverse stress distribution in the core region (photoelastic effect) and a modification of the fiber geometry (waveguide geometry effect) is not enough to split a peak of an FBG. But externally applied stresses what is called transverse residual stress can lead to induced birefringence through the photoelastic effect. In this paper, we concentrated on the induced birefringence when embedding in a variety of composites.

If the modes traveling along the slow axis ($\lambda_{B,2}$) and the fast axis ($\lambda_{B,3}$) about the axes orientation of optical fiber in Fig. 2 have almost same propagation constants, the exchange of power between them is very easy. Therefore, the reflected spectrum has one peak overlapped each other that is the Bragg wavelength (λ_B). However, when the optical fiber shows birefringence, an x-polarized excitation results in wave propagation with a different specific phase shift β compared to a y-polarized excitation. In other word, the x-polarized (β_x) and y-polarized (β_y) LP_{01} mode don't have the same propagation constant any longer when the optical fibers exhibit some ellipticity of the core and/or some anisotropy in the refractive index distribution due to anisotropic stresses in the region including a grating. Therefore, a reflected FBG spectrum has two peaks and the two axes of optically anisotropic medium. This means that it is difficult and ambiguous to process signals for measurement of dynamic strains real-timely because birefringence at the region built in gratings lead to perturbations of the SOP.

In practice, we have experienced many induced

birefringence problems except the case embedded parallel to reinforced fiber of Graphite/Epoxy composite.

3. EXPERIMENT and RESULT

Embedding characteristics

When an optical fiber built in FBG is embedded into some composite structures, it is necessary to observe minutely embedding environments of optical fiber, as well as changes of reflected spectrum of embedded FBG due to residual stresses after cure processing.

We embedded optical fibers parallel ($[0_5/\{0\}/0_5]$ - Case I) and perpendicular ($[90_5/\{0\}/90_5]$ – Case II) to unidirectional reinforced fiber of Graphite/Epoxy composite laminates. And we embedded optical fibers to plain-woven fabric of Glass/Epoxy composite laminates. In case of unidirectional reinforced composite laminates, the thickness of its prepreg was 0.125 *mm* . In case of plain-woven fabric composite laminates, the environments surrounding an optical fiber were quite different to the unidirectional cases because of yarn structure. One yarn of CaseIII ([4plies /{OF}/4plies]) was composed of about 200 E-glass fibers and the thickness of a prepreg is 0.18 *mm* . One yarn of Case IV ([3plies/{OF}/3plies]) was composed of about 600 E-glass fibers and the thickness of a prepreg was 0.22 *mm* (see Fig. 3a, Fig. 4a and Fig. 4b). Each diameter of a bare optical fiber (OF), a graphite fiber and a glass fiber was 125 μm , 7 μm and 10 μm , respectively.

Residual stress has been recognized in conventional thermosetting composites. The residual stress of transverse direction (σ_2) with respect to optical fiber can induced the birefringence phenomenon except the Case I (see Fig. 3c) and also these birefringence effects caused the unique Bragg condition break down in the Case II and the Case III with striped FBGs, and even produced two very distinct Bragg wavelengths in the CaseIII (see Fig. 3d and Fig. 4c). The transverse residual stress that makes un-welcomed effects on the signal processing to measure dynamic strain comes from the internal stress that is induced during composite part processing. This stress builds up due to the shrinkage of the polymetric matrix around the reinforcement. The two main components that contribute to this stress are:

(1) The volumetric shrinkage of the resin during cure processing
(2) The mismatch in the coefficients of thermal expansion of the matrix and the reinforcement.

Related to transverse stress, the Case I and CaseII with only unidirectional prepregs were chosen to distinguish the volumetric shrinkage effects of the resin. And the CaseIII with plain-woven fabric prepregs was chosen as the case with severe residual stresses. In general, the plain-woven fabric laminates have even greater residual stresses after cure processing because of higher volumetric shrinkage due to smaller fiber volume fraction and the mismatch in the CTE of the matrix and the perpendicularly crossed fibers.

To provide an understanding of the cure processing from the viewpoint of transverse residual stress inducing birefringence and the mechanical embedding environments, we inspected the optical fibers embedded in 4 types of specimens at the polishing cross sections (see Fig. 5d ~ 5h). These micrographs help us to understand the various characteristics of the embedded optical fibers. The Case I shown Fig. 5d had the reliability of signal in spite of the shrinkage of resin in the perpendicular direction with respect to the graphite fibers and the optical fiber. As mentioned in the above chapter, the exchange of power between the two modes is very easy in the case of low birefringence induced by small transverse stress. Therefore, the reflected spectrum has one peak overlapped each other. In general, the CaseII has smaller transverse stress in the parallel direction with respect to the graphite fibers because the degree of the fiber shrinkage is much smaller than that of the resin shrinkage. But the reliability of the sensor signal broke down in the CaseII unexpectedly. We can find the cause about this unexpected phenomenon in Fig. 5e. The bare optical fiber embedded perpendicular to the reinforced fibers has resin rich regions in both sides adjacent to the embedded optical fiber. And these resin rich regions induce the additional transverse residual stresses. Therefore FBGs embedded perpendicular to reinforced fibers become to lose the reliability as a dynamic strain sensor. In other words, the cause of the birefringence in the CaseII was not residual transverse stress inside the composite laminate but resin rich region induced by embedding the 125 μm optical fiber. Fig. 5f shows the cross section around the bare optical fiber in the CaseIII. The cause of the higher birefringence in the CaseIII with bare optical fiber is that the Glass/Epoxy plain-woven fabric laminate has even higher residual transverse stress than only unidirectional composite laminate. The greater residual transverse stress occurs due to the severe mismatch in the CTE of the resin and the cross reinforcements, and due to the higher volumetric shrinkage of the resin because of the smaller fiber volume fraction. But the Case III with an acrylate coating optical fiber had no birefringence phenomenon. We can realize this cause for the first time after making observation of the cross section of the Case III with acrylic coating optical fiber. The double acrylic coating of optical fiber shown in Fig. 5g became an elliptic shape due to temperature and pressure during the cure processing. There were small spaces between coating and optical fiber. This space was named as the coating void in this paper. The coating voids generally occupied about 40%~50% of the circumference of the bare optical fiber in the collection of samples. In the case that was recoated by the same material (acrylate), these recoating also protected optical fiber from residual transverse stress lest the reflected spectrum should be split in two peaks. The optical fiber in the Case IV was also safe because the recoating protected a bare optical fiber from transverse stresses as shown in Fig. 5h.

In the second place, we focused on the question that bare optical fibers and coated optical fibers under uneven embedding environments with different microbendings according to each case would have the reliability mechanically after cure processing. Commonly, microbendings cause light losses and backscatters optically and may lead to stress fractures mechanically. In the application of FBG embedded in

composites aspect, mechanical microbending effects are more important than optical microbending effects relatively. At first, we inspected the mechanical microbending of the embedding environments inside the Case II, III and Case IV in the Fig 5a, 5b and 5c by embedding very thin Teflon films. The embedding environment of the Case II shown in the Fig. 5a was even, compared to the Case III and IV. There is a bare optical fiber under this embedding environment in the Fig. 5i and it remained straight and safe mechanically because of its higher Young's modulus than those of fibers and resin. But the embedding environments of the CaseIII and Case IV were very uneven. The height and width of a typical knoll of the CaseIII as shown in Fig. 5b were 0.04 mm and 0.8 mm. There is a bare optical fiber under embedding environment of the Case III in the Fig. 5j. The optical fiber pushed the knolls of yarns and made the interface straight between host composite material and optical fiber. Although these microbendings might induce the power loss on the reflected spectrum after the cure processing, the bare optical fiber remained straight and safe mechanically. In the Case IV, however, the height and width of a typical knoll mounted up to 0.08 mm and 0.9 mm in Fig. 5c and a bare optical fiber failed in each ridge of knoll mechanically because of big yarn structure (see Fig. 5k). Although there were coating voids in the Case III and IV with acrylate coating, the coatings shown in Fig. 5g, 5l, 5h and 5m protect bare optical fibers against microbending failures mechanically. These four micrographs also indicate that though the cure temperature (130°C) was close to the breakdown temperature of the acrylate coating (150°C), the coatings survived during the cure processing except left and right sides of the coatings that were melted to be out of shape.

Consequently, the reliability as both optical fibers and sensors depended on the orientation of optical fiber relative to the reinforced fibers and whether there was the coating or not. The recoating of stripped FBG was very important for the purpose of relieving birefringence optically and microbending effects mechanically when optical fiber with Bragg grating embedded between composite prepregs.

Cure monitoring by WSFL

We performed the cure monitoring in order to observe the history of FBG spectrum during all the cure processing. In this experiment, stripped FBGs were coated again using the recoating instrument. And it was possible to monitor the cure processing of composite materials without any special treatment by WSFL and DPO despite of serious microbending problems of an autoclave. The use of WSFL made these experiments possible because the average output power ($2.22\,mW$) of the WSFL used in this study was very high. A stripped FBG sensor and a recoated FBG sensor were embedded between adjacent plies of the 8-plies plain-woven fabric composite specimens similar to Fig. 3b.

Fig. 7 and Fig. 8 show the change in spectrum obtained by the two type embedded FBG sensors during the typical cure cycle in Fig. 6. From the spectra shown in Fig. 7, we can find the onset time when one peak of the stripped FBG is split into two distinct peaks (Fast axis and slow axis). Before the cooling step, the spectra of the stripped FBG remained unchanged in spite of the curing pressure application. This means that cure pressure (σ_3) is not enough to induce the birefringence phenomenon. After eliminating the cure pressure (6 *atm* = 607.95 *KPa*), the transverse stress was promoted by the thermal contraction of epoxy and the mismatch in the CTE of the epoxy and the perpendicularly crossed fibers in the cooling step. Therefore one clear and definite additional peak appeared at the birefringence onset time (about 182 *min* after starting the cure processing) in the middle of the cooling step. But the additional peak did not appear in the spectra of the recoated FBG as shown in Fig. 8. This means that the recoating protected the FBG sensor from birefringence induced by the transverse stress (σ_2) since the cooling step and microbendings increased by the curing pressure application (σ_3) before the cooling step. As a result of these experiments, we could come to a conclusion that this recoating method is useful in the case of FBG for measurement of dynamic strain of a composite structure.

4. CONCLUSION

Once a composite is cured, an embedded FBG sensor is used to provide the information about the mechanical changes such as strain, natural frequency and so on. Therefore we inspected the embedding environments and birefringence phenomena of optical fibers embedded into composite laminates by microscope analysis and by cure monitoring about change of FBG spectrum. The cure monitoring of plain-woven fabric composites with the striped FBG and the recoated FBG provided comprehensive understandings about the birefringence effect induced by the transverse residual stress. These results allowed detecting the birefringence onset time in the case of birefringent FBG and let us know the usefulness of recoating method in the case of FBG as dynamic strain sensor.

ACKNOWLEDGEMENT

The authors would like to thank the Ministry of Science and Technology, Korea, for the financial by a grant from the Critical Technology project.

REFERENCE

(1) Dunphy, J.R., Meltz, G., Lamm, F.P., and Morey, W.W. "*Multi-function, distributed optical fiber sensor for composite cure and response monitoring*", Proc. SPIE 1370, pp 116-118, 1990.

(2) W.W. Morey, Dunphy, J.R. and Meltz, "*Multiplexing Fiber Bragg Grating sensors*", Proc. SPIE 1586, 1991

(3) C.Y. Ryu, C. S. Hong, "*Development of fiber Bragg grating sensor system using wavelength-swept fiber laser*", Smart Mater. Struct. submitted

(4) Koo, B.Y, Ryu, C.Y., Hong, C.S. and Kim, C.G, "*Vibration and Mode Sensing of a Composite Beam Using Fiber Bragg Grating Sensor Array*" Proc. ACCM, 2000.

(5) Dunphy. J.R., et al., United States Patent 5,399,854, March 21, 1995

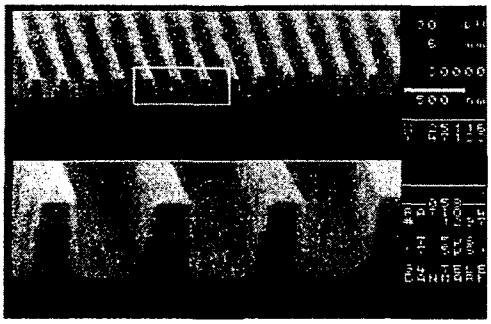

Fig. 1 Phase mask for fabrication of FBG

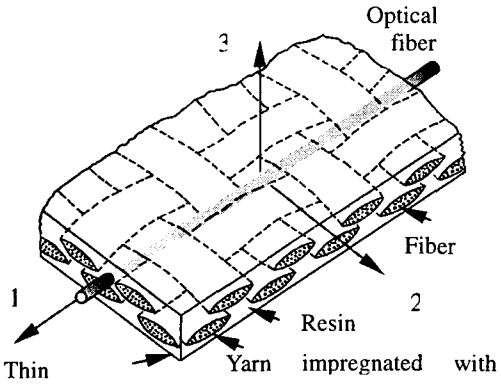

Fig. 2 Axes orientation of a thin composite laminate with an optical fiber

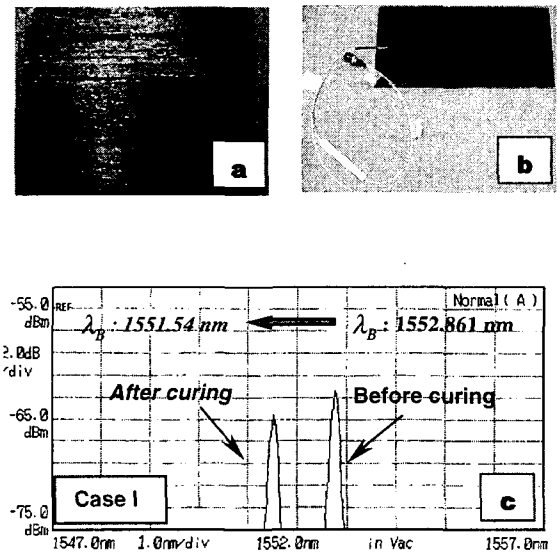

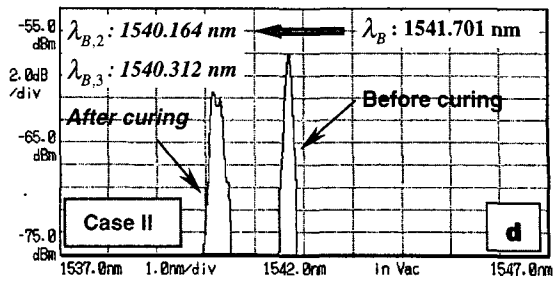

Fig. 3 Configurations and reflected spectra of the Case I and Case II: a) Graphite/Epoxy unidirectional prepreg of the Case I and Case II, b) Specimen of the Case II, c) Reflected FBG spectra of the Case I before and after cure processing, d) Reflected FBG spectra of the Case II before and after cure processing (by LED-OSA system)

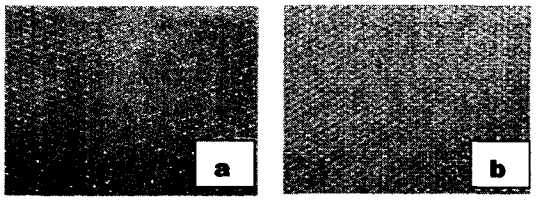

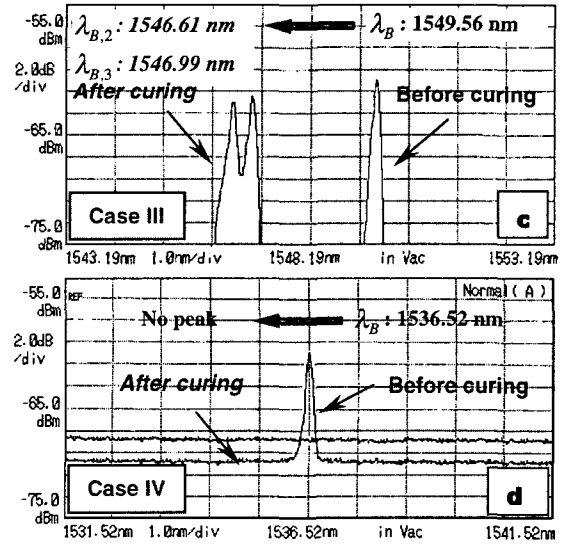

Fig. 4 Configurations and reflected spectra of the Case III and Case IV: a) Glass/Epoxy plain-woven fabric prepreg of the CaseIII, b)Glass/Epoxy plain-woven fabric prepreg of the CaseIV(with bigger yarns), c) Reflected FBG spectra of the CaseIII before and after cure processing, d) Reflected FBG spectra of the CaseIV before and after cure processing (by LED-OSA system).

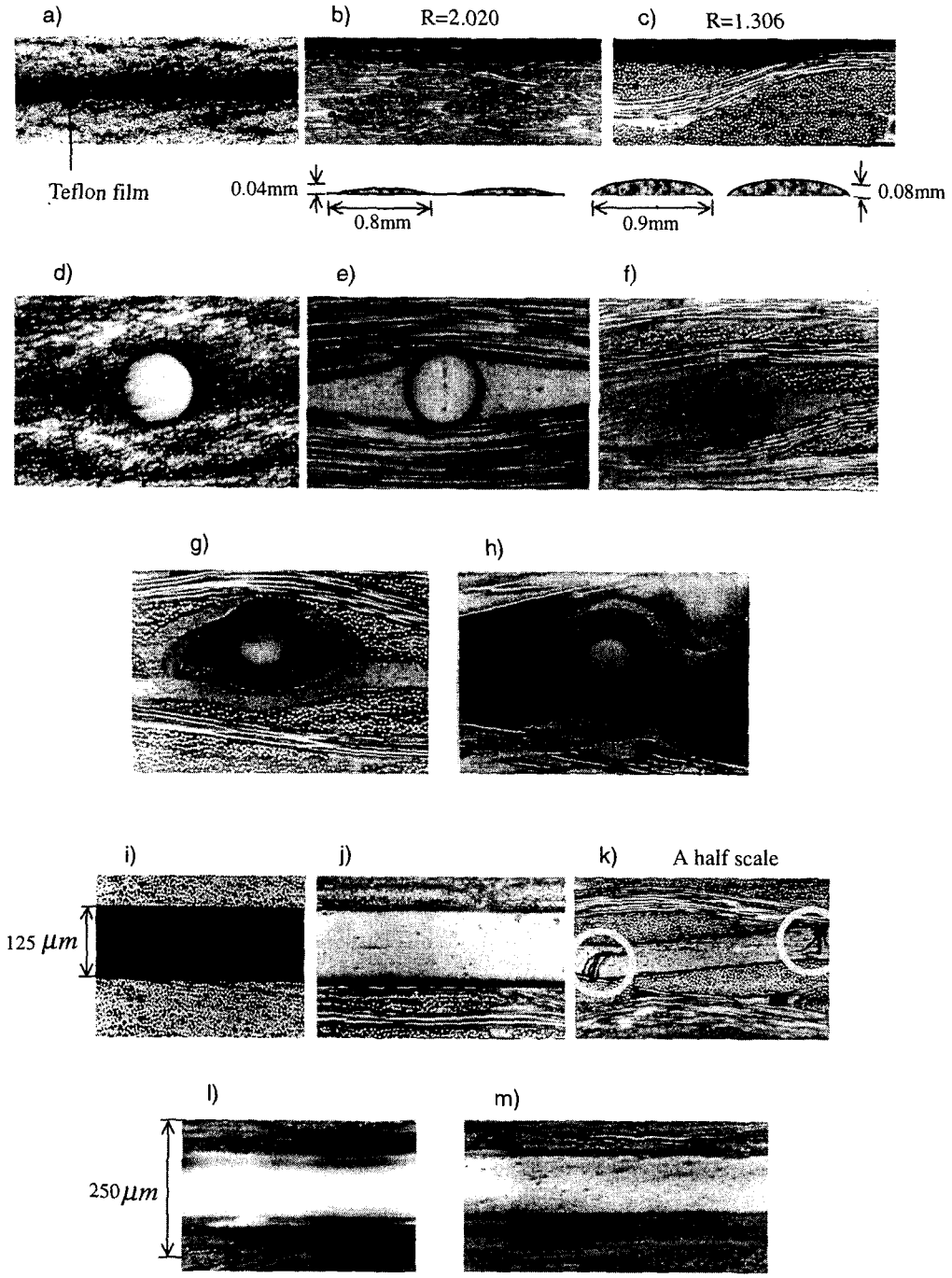

Fig. 5 Embedding environments and optical fibers embedded in 4 –type composite laminates: a), b) and c) Embedding environments of the Case Ⅱ, Ⅲ and Ⅳ, d) Cross section of bare optical fiber in the Case Ⅰ, e) Cross section of bare optical fiber in the Case Ⅱ, f) Cross section of bare optical fiber in the CaseⅢ, g) Cross section of optical fiber with double acrylic coating in the CaseⅢ, h) Cross section of optical fiber with double acrylic coating in the CaseⅣ, i) Side section of bare optical fiber in the Case Ⅱ, j) Side section of bare optical fiber in the CaseⅢ, k) Side section of bare optical fiber in the CaseⅣ, l) Side section of optical fiber with double acrylic coatings in the CaseⅢ, m) Side section of optical fiber with double acrylic coating in the Case Ⅳ

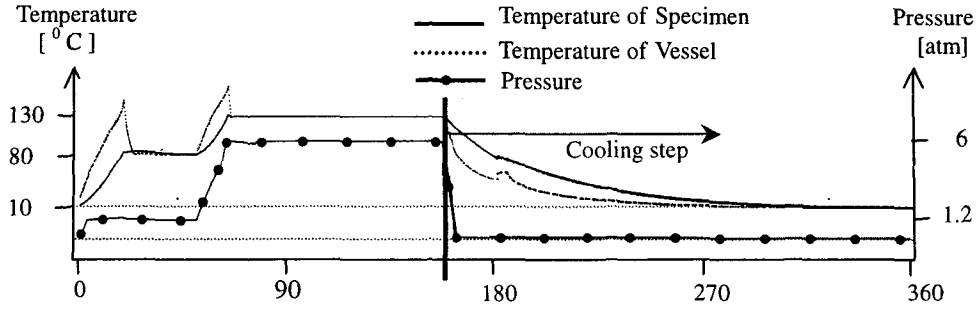

Fig. 6 Typical cure cycle of the vacuum bag mold process

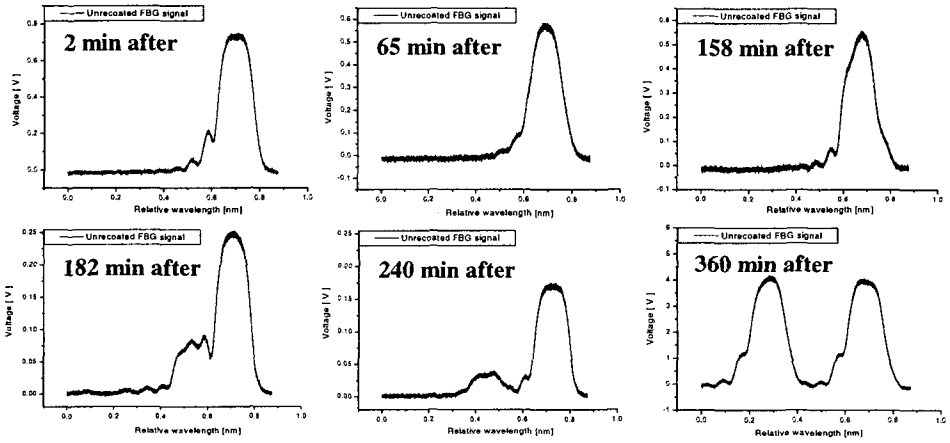

Fig. 7 Change in spectrum of striped FBG related to birefringence during the vacuum bag mold process

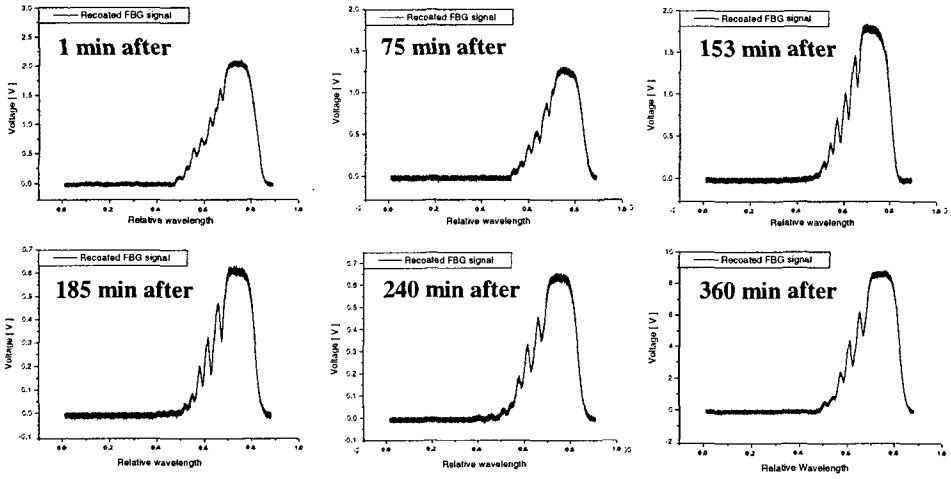

Fig. 8 Change in spectrum of recoated FBG related to birefringence during the vacuum bag mold process